The EMBO Journal vol.15 no.1 pp.125–134, 1996

Solution structure of the ETS domain from murine Ets-1: a winged helix–turn–helix DNA binding motif

Logan W.Donaldson, Jeannine M.Petersen[1], Barbara J.Graves[1] and Lawrence P.McIntosh[2]

Department of Biochemistry and Molecular Biology and Department of Chemistry, University of British Columbia, Vancouver, British Columbia, Canada V6T 1Z3 and [1]Department of Oncological Sciences, Division of Molecular Biology and Genetics, University of Utah School of Medicine, Salt Lake City, UT 84132, USA

[2]Corresponding author

Ets-1 is the prototypic member of the *ets* family of transcription factors. This family is characterized by the conserved ETS domain that mediates specific DNA binding. Using NMR methods, we have determined the structure of a fragment of murine Ets-1 composed of the 85 residue ETS domain and a 25 amino acid extension that ends at its native C-terminus. The ETS domain folds into a helix–turn–helix motif on a four-stranded anti-parallel β-sheet scaffold. This structure places Ets-1 in the winged helix–turn–helix (wHTH) family of DNA binding proteins and provides a model for interpreting the sequence conservation of the ETS domain and the specific interaction of Ets-1 with DNA. The C-terminal sequence of Ets-1, which is mutated in the v-Ets oncoprotein, forms an α-helix that packs anti-parallel to the N-terminal helix of the ETS domain. In this position, the C-terminal helix is poised to interact directly with an N-terminal inhibitory region in Ets-1 as well as the wHTH motif. This explains structurally the concerted role of residues flanking the ETS domain in the intramolecular inhibition of Ets-1 DNA binding.

Keywords: DNA binding/intramolecular inhibition/protein NMR structure/selective labelling/winged helix–turn–helix

Introduction

Most transcriptional regulatory proteins function by specifically recognizing promoter or enhancer DNA sequences. The large number of transcription factors that orchestrate the genetic programme of an organism display a relatively small set of DNA binding motifs. Nevertheless, the DNA binding activities of transcription factors bearing a common motif can differ, recognizing a diverse set of sequences with a wide range of affinities. To some extent, this diversity is specified by the minimal DNA binding domain. In other cases, post-translational modification, ligand binding, oligomerization, intermolecular associations and intramolecular contacts influence their DNA binding activities. A key step in understanding both sequence-specific DNA binding and additional layers of regulation of a particular transcription factor is the knowledge of the three-dimensional structure of its DNA binding motif.

Since its initial identification as an essential transforming activity of avian erythroblastosis virus E26 (Leprince *et al.*, 1983; Nunn *et al.*, 1983), the *ets* gene family has emerged as a widespread class of transcription factors involved in many aspects of cellular growth and differentiation. A highly conserved DNA binding motif, termed the ETS domain, characterizes this family and confers specificity toward promoter sequences containing a common 5′-GGA(A/T)-3′ core motif (for reviews, see Karim *et al.*, 1990; Macleod *et al.*, 1992; Janknecht and Nordheim, 1993; Wasylyk *et al.*, 1993). The similarity of these DNA recognition sites suggests the need for additional regulatory mechanisms. Indeed, both intermolecular and intramolecular interactions have been shown to modulate DNA binding by ETS domain proteins. Partnerships between *ets* proteins and transcription factors belonging to other structural families have served to establish general principles for cooperative protein–protein interactions in the control of gene expression (Thompson *et al.*, 1991; Pongubala *et al.*, 1992; Janknecht and Nordheim, 1993; Wasylyk *et al.*, 1993). In addition, the intramolecular regulation of DNA binding by Ets-1 has emerged as a model for the phenomenon of autoinhibition (Hagman and Grosschedl, 1992; Leprince *et al.*, 1992; Lim *et al.*, 1992; Wasylyk *et al.*, 1992; Fisher *et al.*, 1994; Petersen *et al.*, 1995). The negative regulation by intramolecular interactions appears to be lost in v-*ets*, the transforming oncogenic version of *ets-1* found in the avian leukosis virus E26 (Leprince *et al.*, 1983; Nunn *et al.*, 1983; Nunn and Hunter, 1989; Hahn and Wasylyk, 1994).

We have shown recently that the ETS domain of Ets-1 adopts a secondary structure remarkably similar to DNA binding motifs belonging to the winged helix–turn–helix (wHTH) structural family (Donaldson *et al.*, 1994). The NMR-derived tertiary structure of the related *ets* protein Fli-1 (Liang *et al.*, 1994a,b) has reinforced the similarity of the ETS domain to the DNA binding domains of the wHTH proteins *Escherichia coli* CAP (Schultz *et al.*, 1991) and biotin repressor BirA (Wilson *et al.*, 1992), histone H5 (Ramakhrishnan *et al.*, 1993), hepatocyte nuclear factor HNF-3γ (Clark *et al.*, 1993), heat shock factor HSF (Damberger *et al.*, 1994; Harrison *et al.*, 1994; Vuister *et al.*, 1994a,b), μ-transposase (Clubb *et al.*, 1994), LexA (Fogh *et al.*, 1994), replication terminator protein RTP (Bussiere *et al.*, 1995) and diptheria toxin repressor DtxR (Qiu *et al.*, 1995). As demonstrated in both crystallographic and NMR studies, the wHTH proteins contain a three helix bundle with a helix–turn–helix (HTH) motif that makes specific contacts to the major groove of DNA. An anti-parallel β-sheet forms a scaffold against which these helices pack. The term wHTH highlights the role of the β-sheet and associated wing-like loops in the structure

of the binding domain as well as in possible DNA interactions. At the same time, it distinguishes these proteins from others that use only a HTH DNA binding motif (Brennan, 1993; Clark *et al.*, 1993).

Here we report the NMR-derived tertiary structure of Ets-1ΔN331, an N-terminal deletion mutant of murine Ets-1. This 110 residue protein contains the 85 residue ETS domain and a 25 residue extension that ends at the native C-terminus of Ets-1. The global fold of the ETS domain, with three α-helices packed on a four-stranded anti-parallel β-sheet, confirms the placement of Ets-1 in the wHTH family. This structure provides a framework for interpreting the sequence conservation in the ETS domain and leads to a model for sequence-specific DNA binding by Ets-1. The C-terminal tail contains a fourth α-helix that contributes to the structure of Ets-1ΔN331 by packing against the ETS domain. This helix is positioned to interact with inhibitory sequences immediately N-terminal to the ETS domain in the native protein. This proposed interaction provides a structural basis for the concerted role of the sequences flanking the N- and C-terminus of the ETS domain in the autoinhibition of DNA binding by Ets-1.

Results

Spectral assignments

Ets-1ΔN331 is a minimal fragment of Ets-1 that is fully functional for DNA binding and displays a set of base and sugar phosphate contacts similar to that observed for the full-length protein (Petersen *et al.*, 1995). The assignments of the main chain resonances of uniformly ^{15}N- and ^{13}C-labelled Ets-1ΔN331 were reported previously (Donaldson *et al.*, 1994). These led to the determination of the secondary structure of the protein based on NMR chemical shifts, nuclear Overhauser effects (NOE) and J-coupling restraints, and amide hydrogen exchange kinetics. To determine the tertiary structure of the protein, the resonances from the side chain aliphatic nuclei of Ets-1ΔN331 were assigned using three-dimensional (3-D) ^{1}H-^{13}C and ^{1}H-^{13}C-^{15}N NMR experiments. Complete correlations were not detected between the ^{13}C or ^{1}H nuclei of several residues with long side chains, due to the limited solubility and generally broad resonances of Ets-1ΔN331. The methyl groups of the 4 valine and 13 leucine residues were assigned stereospecifically using the elegant approach of fractional ^{13}C-labelling (Neri *et al.*, 1989). The identities of the remaining methyl groups in Ets-1ΔN331 were confirmed by the ^{13}C coupling patterns observed in the ^{1}H-^{13}C HSQC spectrum of the fractionally labelled protein, as summarized by Szyperski *et al.* (1992).

Ets-1ΔN331 contains 17 aromatic residues. The proton resonances of the aromatic rings were identified using homonuclear DQF-COSY, TOCSY and NOESY experiments recorded on three samples of Ets-1ΔN331 in which two of either tryptophan, tyrosine or phenylalanine were deuterated selectively (McIntosh *et al.*, 1990). The combination of spectral simplification due to isotope labelling by residue type with the high signal-to-noise and resolution of 2-D NMR spectroscopy was invaluable, providing an avenue for spin system assignment as well as for resolving the NOE interactions to each type of aromatic amino acid.

Structural restraints

The tertiary structure of Ets-1ΔN331 was determined using experimental data derived from three sources. (i) The backbone φ dihedral angles of 77 residues were restrained based on their $^{3}J_{HN\text{-}H\alpha}$ coupling constants, as measured with the HMQC-J experiment (Kay and Bax, 1990). (ii) Main chain hydrogen bonds were identified for the 29 residues that were significantly protected from amide hydrogen exchange and exhibited NOE, $^{3}J_{HN\text{-}H\alpha}$ and secondary chemical shift patterns indicative of their involvement in regular α-helical or β-sheet secondary structures (Donaldson *et al.*, 1994). (iii) Qualitative NOE distance restraints were obtained from 3-D ^{15}N- and ^{15}N/^{13}C-resolved NOESY spectra recorded with 50–150 ms mixing periods. Many critical long distance restraints involving aromatic protons were also obtained from 2-D ^{1}H-^{1}H NOESY spectra recorded on samples of Ets-1ΔN331 with selectively deuterated aromatic rings. After an iterative cycle of structure calculations and NOESY spectral assignments, a total of 229 intraresidue, 383 short range and 123 long range (>4 residues apart) distance restraints were used to determine the final ensemble of Ets-1ΔN331 structures.

Of the 50 structures derived from an initial simulated annealing stage, 20 with acceptable energies and no distance violations (>0.5 Å) or torsion angle violations (>5°) were selected for additional refinement. The mean minimized structure of Ets-1ΔN331 was calculated by averaging the coordinates of the individual structures, aligned to each other using the backbone atoms of residues 336–377, 386–396, 401–405 and 411–435, followed by restrained regularization. The best fit superimposition of the ensemble of 20 simulated annealing structures determined for Ets-1ΔN331 is presented in Figure 1. The number of ^{1}H assignments and NOE restraints per residue, the root mean square (r.m.s.) deviations of the C^{α} atom positions about the mean minimized structure, and the angular order parameters, Sφ and Sψ, are shown in Figure 2.

Excluding disordered sequences, the ensemble of Ets-1ΔN331 structures has average r.m.s. deviations versus the mean minimized structure of 1.65 Å for all remaining backbone (N, C^{α}, C′ and O) atoms and 1.34 Å for backbone atoms in the helices and strands. This degree of precision is attributable directly to the limited solubility of the Ets-1 fragment (<0.8 mM), the need to use high ionic strength conditions (500 mM NaCl) and the effects of internal motions on a millisecond timescale (Donaldson *et al.*, 1994).

Structural features

Ets-1ΔN331 is composed of four α-helices (H1 337–345, H2 369–377, H3 386–396, and H4 428–434) packed against a four-stranded anti-parallel β-sheet (S1 354–357, S2 362–365, S3 402–405, S4 411–414). This is in agreement with the secondary structure reported previously for Ets-1ΔN331, with a minor difference in the definition of the C-terminal boundary of helix H2 (Donaldson *et al.*, 1994). The three helices (H1–H3) and the four β-strands in the ETS domain are well defined, with low r.m.s. deviations and angular order parameters approaching unity. The C-terminal boundary of helix H3 is uncertain because the signal-to-noise ratio from residues

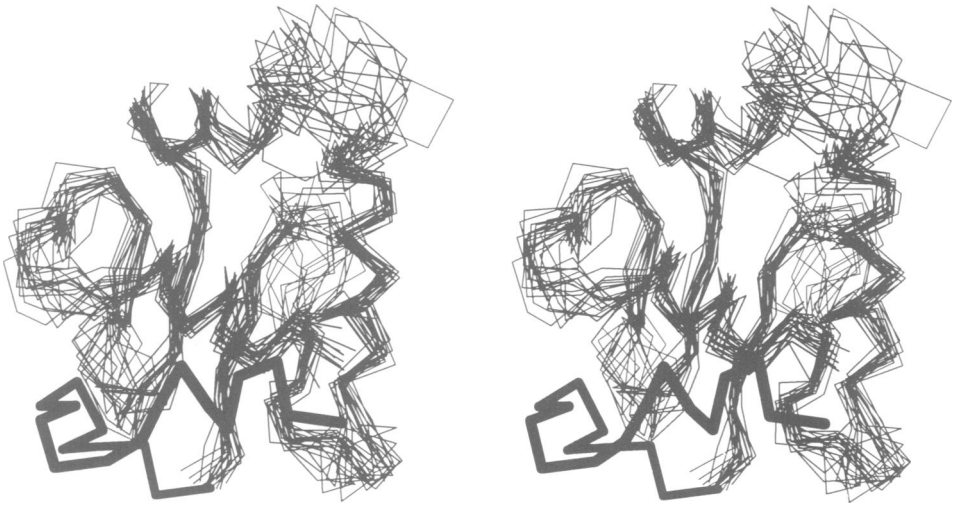

Fig. 1. Ets-1ΔN331 is composed of a wHTH motif and C-terminal α-helix. The stereoview shows 20 simulated annealing structures of Ets-1ΔN331 superimposed on the backbone atoms of residues 336–377, 386–396, 401–405 and 411–435. For clarity, only the average, minimized structure (thick bar) is shown for residues 416–436. The N-terminal four residues (331–334) are disordered and were not included in the structure calculations.

396–399 is poor due to conformational averaging (Donaldson *et al.*, 1994). Residues 428–434 in the C-terminal extension form the fourth helix, H4. The r.m.s. deviations of the residues in this helix versus the mean minimized structure are larger than observed with the first three helices (Figure 2C) yet, independently, backbone atoms of residues 428–434 superimpose with an r.m.s. deviation of 0.66 Å. The angular order parameters of these residues also approach unity. Therefore, the conformation of helix H4 is defined well locally, while the position of this helix relative to the remainder of Ets-1ΔN331 is not established precisely. This is due in part to extensive chemical shift degeneracy in the region of Thr425–Val435. In contrast, low angular order parameters and high r.m.s. deviations for residues in the turns or loops linking H1/S1, H2/H3, H3/S3 and S3/S4, as well as the termini of the protein, show that these regions are disordered in the ensemble of calculated structures due to a limited number of NMR restraints or conformational flexibility.

Discussion

The ETS domain: a wHTH motif

Using NMR methods, we have determined the solution structure of Ets-1ΔN331, a 110 amino acid deletion mutant of murine Ets-1. Ets-1ΔN331 is a high affinity DNA binding protein composed of the 85 amino acid ETS domain (Gly331–Val415) and the native 25 amino acid C-terminal sequence of Ets-1 (Cys416–Asp440). The global fold of the ETS domain consists of a HTH motif packed on a four-stranded anti-parallel β-sheet scaffold. A fourth helix, H4, located in the C-terminal tail, is packed anti-parallel to H1.

A comparison of the secondary and tertiary structural elements of Ets-1ΔN331 establishes the murine Ets-1 ETS domain as a member of the wHTH family of DNA binding proteins. Figure 3 presents ribbon diagrams of the DNA binding domains of CAP, HSF and HNF-3γ, along with that of Ets-1. The common fold of three α-helices on an anti-parallel β-sheet that defines the wHTH motif is

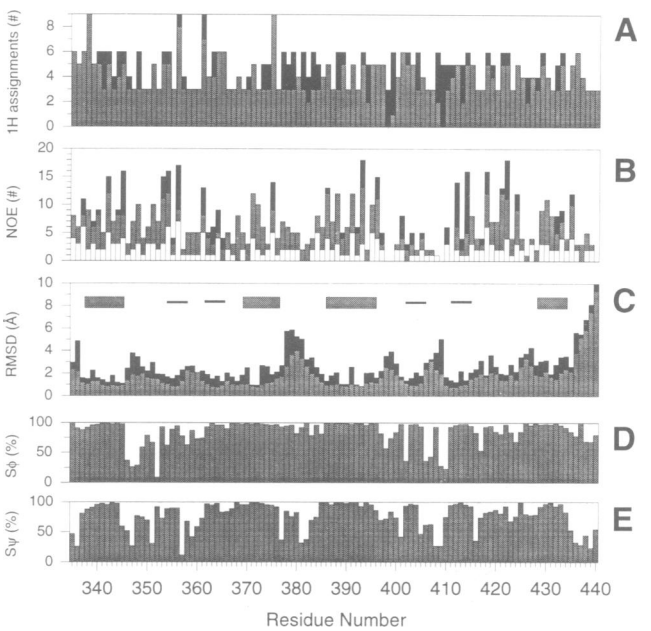

Fig. 2. Summary of NMR restraints and structural parameters for Ets-1ΔN331. (**A**) The number of restraints depends on the extent of spectral assignments for a given residue. Solid bars indicate the maximum number of proton assignments expected per residue, while grey bars indicate the actual number of assignments made. Methylene and symmetrically related aromatic protons are counted only once. (**B**) Total number of intraresidue (open), short range (grey) and long range (solid) NOE restraints per residue used to determine the final set of Ets-1ΔN331 structures. All restraints are counted once for each hydrogen involved. (**C**) The r.m.s. deviation of the backbone (grey) and all heavy atoms (solid) for the ensemble of 20 structures of Ets-1ΔN331 aligned against the average, minimized structure. The locations of the four α-helices and four β-strands are indicated by the thick and thin horizontal bars, respectively. (**D** and **E**) The angular order parameters Sϕ and Sψ for the ϕ and ψ main chain dihedral angles, respectively, observed in the ensemble of protein structures. The order parameters reflect the local precision of the structure. The N-terminal residues 331–334 were omitted from the structure calculations.

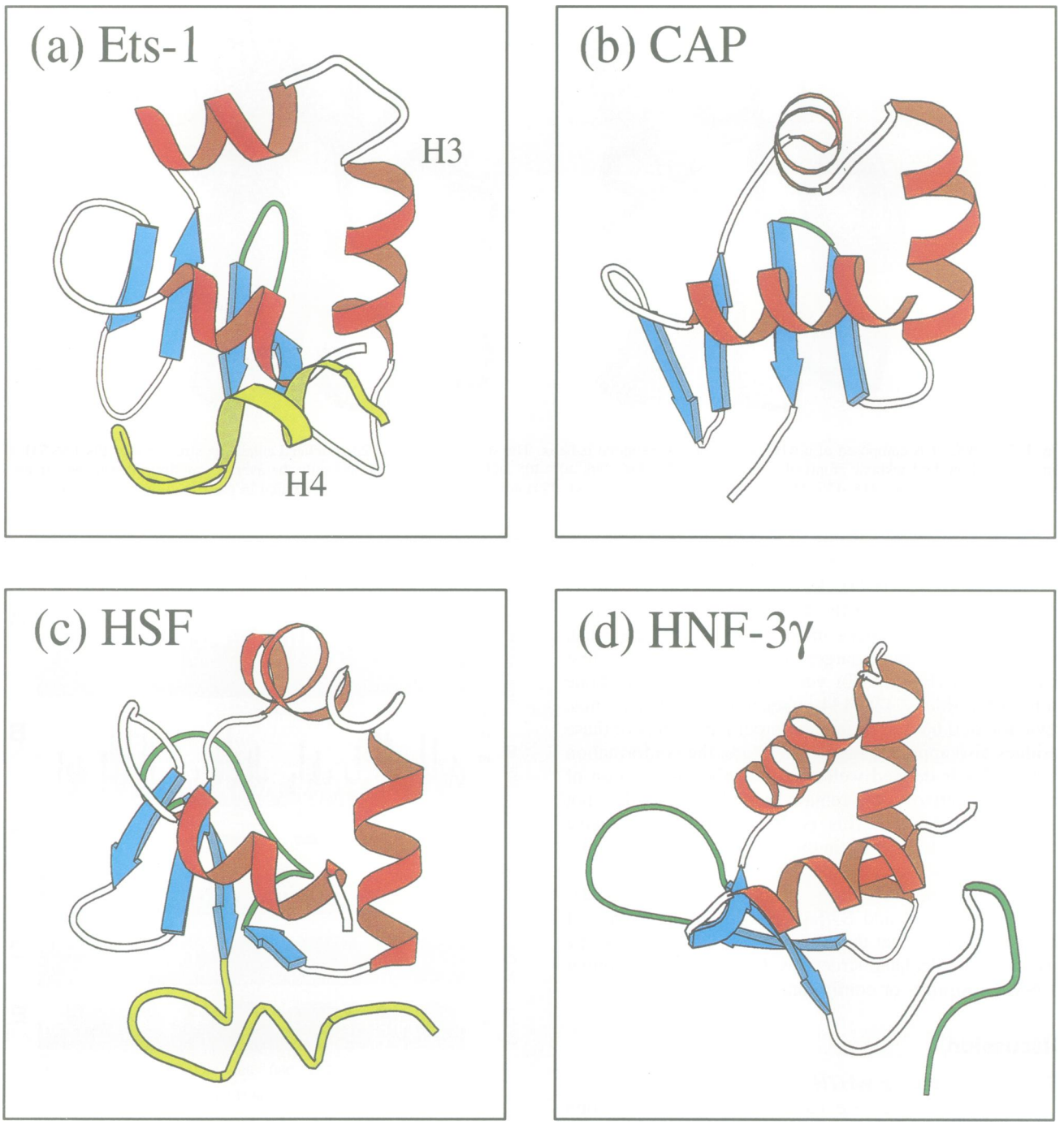

Fig. 3. Ribbon diagrams showing a comparison of the wHTH DNA binding domains of (**a**) murine Ets-1, (**b**) CAP (Schultz *et al.*, 1991), (**c**) *Drosophila* HSF (Vuister *et al.*, 1994b) and (**d**) HNF-3γ (Clark *et al.*, 1993). The wHTH α-helices are red and β-strands blue. Each protein is oriented with helices H1 and H3 in the plane of the page. The HTH motif is formed by helices H2 and H3, with H3 (vertical) being the recognition helix for major groove DNA binding. A distinctive β-hairpin loop or wing (green) makes additional flanking sugar or phosphate contacts in the DNA complexes of CAP, HNF-3γ and the Fli-1 ETS domain (Liang *et al.*, 1994b). The analogous extended loop in HSF does not appear to be involved directly in DNA binding to the heat shock response elements (Hubl *et al.*, 1994; Vuister *et al.*, 1994b). The structures of sequences C-terminal to the DNA binding domains of Ets-1ΔN331, *Drosophila* HSF, and HNF-3γ and are also compared in the figure. In HNF-3γ, this region forms a pronounced second wing (green) and provides additional phosphate and specific minor groove base contacts. In Ets-1, evidence exists for intramolecular association of the C-terminal residues, including helix H4 (yellow), with sequences N-terminal to the ETS domain, resulting in inhibition of DNA binding. The figure was drawn using Molscript (Kraulis, 1991).

clearly evident. This structural similarity was not readily recognized due to the absence of any significant sequence similarity among the various wHTH proteins. However, in light of the tertiary structures of these proteins, a pronounced pattern of aliphatic and aromatic residues contributing to their respective hydrophobic cores can be detected. For example, Leu337, Trp338 and Leu341 (H1), Trp375 (H2), and Leu389 and Leu393 (H3) greatly influence the relative placement of the three helices in the Ets-1 ETS domain. *Kluyveromyces lactis* HSF contains the analogous residues Leu202, Trp203 and Val206 (H1), Phe232 (H2), and Phe249 and Leu253 (H3) (Harrison

et al., 1994). Important residues that establish the interior hydrophobic face of the amphipathic β-sheet in Ets-1 include Ile354 and Trp356 (S1), Phe363 and Leu365 (S2), Ile402 (S3), and Tyr412 and Phe414 (S4) with counterparts in HSF being Ile215 and Trp217 (S1), Ile224 and Val226 (S2), Trp258 (S3), and Trp277 and Phe279 (S4).

Although the wHTH proteins share a common fold, Figure 3 also illustrates the considerable variation that exists in terms of interhelical angles, helix, strand and turn or loop lengths, and the numbers of β-strands. In comparison with interhelical angles summarized previously for several wHTH proteins (Harrison *et al.*, 1994; Vuister *et al.*, 1994b), the Ets-1 ETS domain shows helical crossing angles of 141° for H1/H2, 108° for H1/H3 and 109° for H2/H3. The four residue turn found in the prokaryotic HTH motif, such as CAP, is replaced with eight residues in Ets-1 and HNF-3γ. The wHTH proteins also differ in the number of strands forming the antiparallel β-sheet. The DNA binding domains of Ets-1, CAP and HSF have four strands, HNF-3γ, histone H5, μ-transposase and RTP have three, and BirA, LexA and DtxR only two. In all cases, at least two β-strands follow the HTH motif, providing a loop or wing for possible DNA contacts. A third helix precedes the HTH motif, except in the case of μ-transposase, which forms a distinct class of wHTH proteins by having this helix located after the β-sheet (Clubb *et al.*, 1994). These structural variations undoubtedly reflect the biological diversities exhibited by members of the wHTH family. For example, wHTH proteins function as monomers, dimers or even trimers to specifically, or in the the case of histone H5, non-specifically bind DNA.

Homology among ETS domain sequences

The *ets* family has >20 members from a variety of metazoan species (Lautenberger *et al.*, 1992; Degnan *et al.*, 1993). Relative to Ets-1, these family members show sequence identity within their ETS domains ranging from 96% in the case of Ets-2 to 39% in PU.1. The diagnostic features of the ETS domain include a pattern of conserved hydrophobic residues, highlighted by three essentially invariant tryptophans, and a C-terminal region rich in basic amino acids (Janknecht and Nordheim, 1993; Wasylyk *et al.*, 1993). To investigate the structural basis of this sequence conservation, 15 ETS domains were aligned (Figure 4a) and scored according to an evolutionary mutation matrix at each residue position (Henikoff and Henikoff, 1992). When colour coded on the structure of the Ets-1 ETS domain (Figure 4B), a hydrophobic core involving highly conserved residues from all three helices and four β-strands is readily apparent. Notably, extensive packing contacts are made by the three tryptophans (338, 356 and 375), as well as Phe340, Leu341 and Leu345 in helix H1, Ile354 in sheet S1, Phe363 in sheet S2, Tyr386 and Leu389 in helix H3, and Tyr412 and Phe414 in sheet S4. These residues are essential to maintain the structural integrity of the ETS domain. In contrast, the regions of the highest sequence variability, including amino acid insertions or deletions, map to the loops or turns connecting the α-helices and β-sheets.

The conserved basic amino acids of the ETS domain are found within the HTH motif (helices H2 and H3), the final two strands of the β-sheet, and the loop or wing connecting these strands (Figure 4a and b). As discussed below, these positively charged side chains contribute to the DNA binding interface of the ETS domain. The pronounced conservation of residues in the recognition helix H3 correlates well with the conserved 5′-GGA(A/T)-3′ core sequence found in all regulatory elements bound by *ets* family members.

ETS domains of Ets-1 and Fli-1

The structure of the murine Ets-1 ETS domain is similar to that reported recently for the ETS domain within a 98 amino acid fragment of human Fli-1 (Liang *et al.*, 1994a,b). These two *ets* proteins show 69% sequence identity within their ETS domains. However, the smaller Fli-1 derivative lacks the helical C-terminal extension found in Ets-1ΔN331 and was characterized as a complex with a 16 bp DNA duplex. Therefore, no major changes of secondary structure or global fold arise in the ETS domain due to DNA binding or the presence of the additional C-terminal helix.

Two differences between the structures of Ets-1ΔN331 and the Fli-1 ETS domain bound to DNA are noteworthy. First, the r.m.s. deviations of several regions, such as the turn between helices H2 and H3 of the HTH motif and the loop or wing connecting β-strands S3 and S4, are greater in the ensemble of structures calculated for Ets-1ΔN331 than for the corresponding regions of the Fli-1–DNA complex (Figure 1; Liang *et al.*, 1994b). In addition, the loop between S3 and S4 is positioned farther from the HTH motif in the mean structure determined for Fli-1 relative to that of Ets-1. This, in part, reflects the limited number of NMR restraints used to define the conformations of these regions in Ets-1ΔN331 (Figure 2). However, based on NMR spectral changes associated with DNA complexation as well as protein–DNA NOE interactions, the turn and loop or wing in Fli-1 appear to contribute directly to the binding of the nucleic acid (Liang *et al.*, 1994a,b). Therefore, it is likely that these solvent-exposed regions exhibit conformational flexibility that is restricted upon DNA binding.

Second, the orientation of helix H2 relative to helices H1 and H3 differs in the two structures. This is apparent from the crossing angle of H1 and H2, which is 140° in the Ets-1 ETS domain as compared with 112° in the Fli-1–DNA complex (Liang *et al.*, 1994b). The observed difference in helix packing may result from DNA binding by the Fli-1 ETS domain or the presence of the C-terminal helix H4 in Ets-1ΔN331. Helix H2 forms part of the HTH motif and thus it is possible that a change in the relative orientation of this helix accompanies DNA recognition. Alternatively, the C-terminal helix H4 directly contacts helix H1 in Ets-1ΔN331 and thus may influence the packing of the α-helices within the Ets-1 ETS domain (Figure 1). High resolution studies of the Ets-1 and Fli-1 ETS domains in the free and DNA-bound forms are necessary to establish the reasons for these apparent structural differences.

DNA binding by the Ets-1 ETS domain

Extensive biochemical studies have characterized the interaction between the Ets-1 ETS domain and DNA (Figure 5; Nye *et al.*, 1992). Ets-1 binds DNA as a monomer at sites containing the core recognition sequence,

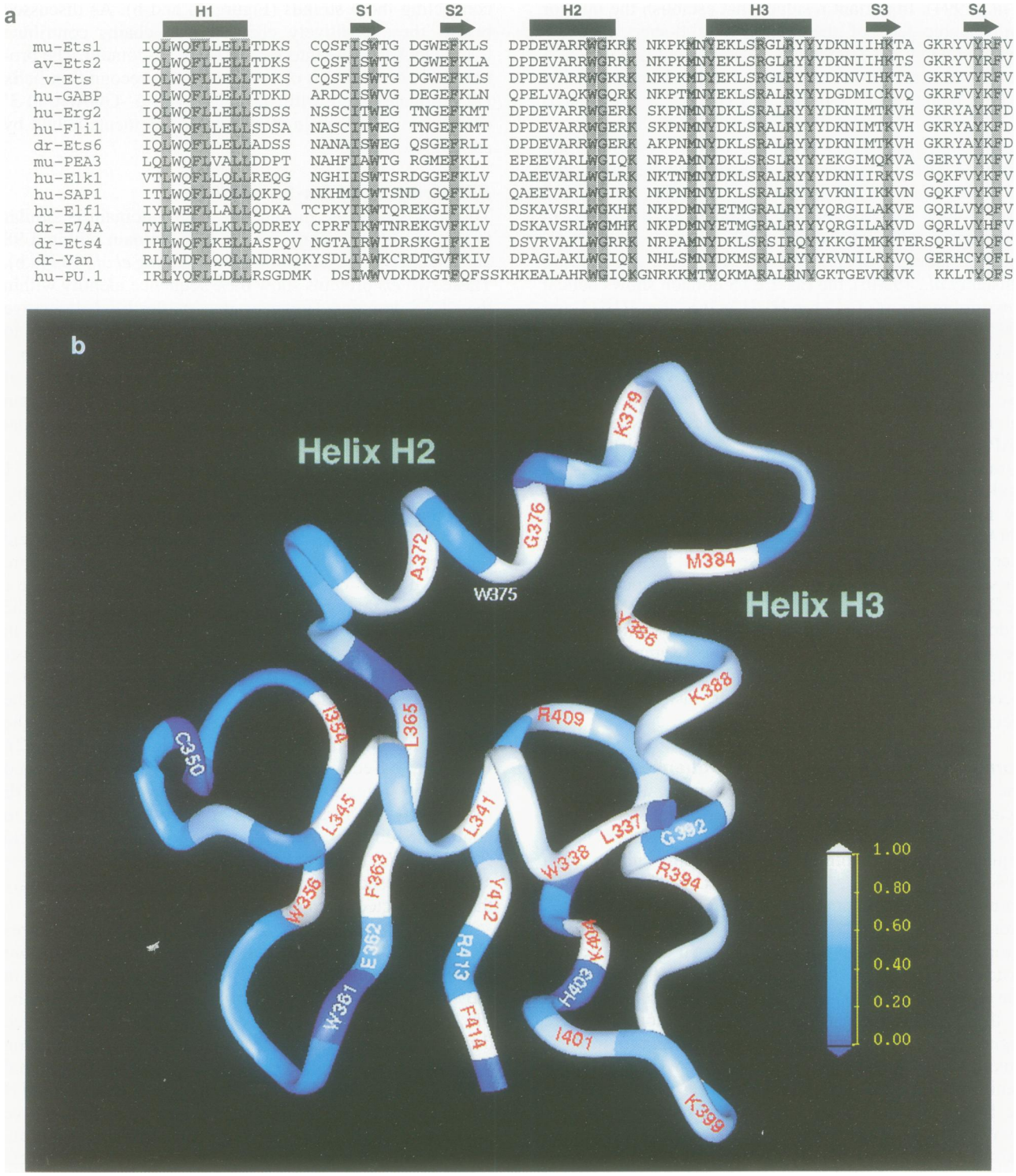

Fig. 4. (**a**) A representative population of 15 ETS domains, aligned in order of descending sequence homology to murine Ets-1. Invariant amino acids are shaded and the secondary structure of Ets-1ΔN331 indicated by boxes (α-helices) and arrows (β-strands). (**b**) The sequences were scored per residue relative to the murine Ets-1 sequence according to a BLOSUM62 evolutionary mutation matrix (Henikoff and Henikoff, 1992). The sequence conservation is presented as a white (most conserved) to blue (least conserved) colour gradient on residues 336–415 of the average, minimized structure murine Ets-1. The figure was generated using the program InsightII (Biosym, Inc.)

5′-GGA(A/T)-3′. Chemical and nuclease protection assays demonstrate that the protein–DNA interactions encompass a relatively large 20 bp region and are localized on one face of the double helix. Alkylation interference experiments implicate a central 9 bp region of close contacts. Consistent with this putative contact region, consensus data show sequence-specific recognition over 9 bp (Fisher *et al.*, 1991; Woods *et al.*, 1992). Guanine methylation interference strongly suggests that Ets-1 recognizes the conserved core GGA sequence in the major

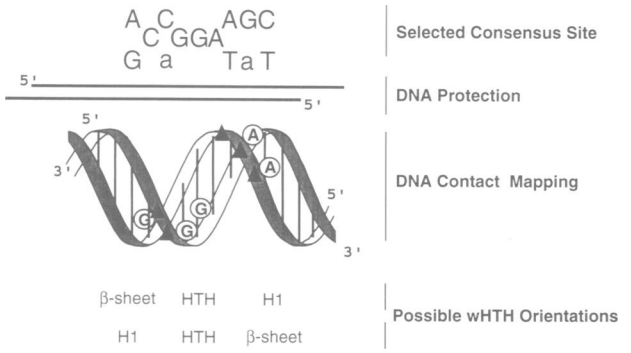

Fig. 5. Summary of the interactions of Ets-1 with DNA and a model for binding by the wHTH motif. DNase I and hydroxyl radical protection data indicate that 20 bp of DNA are affected by Ets-1 binding (Nye *et al.*, 1992). The sequence-specific recognition site spans 9 bp with the invariant core sequence asymmetrically positioned. Backbone contacts detected by ethylation interference are indicated by solid triangles on the DNA helix. Close contacts in the major and minor groove are inferred from interference of binding due to methylation of G and A, respectively. Only the strongest sites of interferences are included in the figure. Two alternative orientations of the asymmetric wHTH motif on the DNA are presented. Elements of the HTH include helices H2, H3 and the H2–H3 turn. H1 refers to the N-terminus of helix H1. The β-sheet includes the loop or wing between S3 and S4 and possibly residues between S2 and the N-terminus of H2.

groove of the DNA. These data demonstrate that the putative interactive surface encompasses a relatively central major groove contact zone flanked by two minor groove interaction regions.

In light of these biochemical studies, it is reasonable to consider a model for the DNA–protein interface. The most definitive aspect of such a model is the interaction of the HTH structure with the conserved core 5′-GGA(A/T)-3′ motif in the major groove of the DNA helix. A variety of genetic analyses are consistent with this interaction (Janknecht *et al.*, 1994; Liang *et al.*, 1994b; Mavrothalassitis *et al.*, 1994), including an altered specificity mutant in helix H3 that changes the recognition of the (A/T) position in the core sequence (Bosselut *et al.*, 1993). A single assigned NOE was reported for the Fli-1–DNA complex that links a specific amino acid to a specific base and brings H3 close to the core sequence (A/T) position (Liang *et al.*, 1994b). Other parts of the structure on the same surface of the ETS domain that are poised to provide additional contacts include the N-terminus of helix H1, the loop connecting strand S2 and helix H2, the eight residue turn between helices H2 and H3, and the loop or wing between strands S3 and S4. Charged or polar residues that could contact either the phosphates or bases are found on all of these elements. In the structures of the binding domains of CAP and HNF-3γ co-crystallized with DNA, the analogous regions of these proteins are observed to interact with the nucleic acid. In the Fli-1–DNA complex, there are unassigned NOEs to DNA from the N-terminus of helix H1, the H2–H3 turn and the S3–S4 loop. Our previous suggestion that the extreme C-terminal region of Ets-1 could be involved in DNA binding (Donaldson *et al.*, 1994) is not consistent with recent data demonstrating that an 85 residue fragment bearing the minimal ETS domain makes contacts on DNA identical with those made by Ets-1 and Ets-1ΔN331 (Q.Xu and B.J.Graves, unpublished observations).

Surprisingly, two alternative orientations of the wHTH motif on the Ets-1 binding site are possible that fit the existing structural and biochemical data as well as mutational analyses. In either orientation, helix H3 of the HTH motif binds DNA in the major groove. The difference between the two models is in the precise orientation or polarity of helix H3 and positioning of helix H1 and the β-sheet with respect to the DNA sequence. In one case the N-terminus of helix H1 would be located over the minor groove, contacting the region 3′ to the GGA core sequence. In the other orientation, this helix would be positioned 5′ to the GGA core sequence.

The ambiguity of the current data could be explained as being due, in part, to a conformational change of the DNA binding site. Two lines of evidence suggest that Ets-1 causes a change in the structure of DNA upon binding. First, Ets-1 binding induces an invariant DNase I-hypersensitive site 3′ to the conserved 5′-TCC-3′ in all Ets-1 recognition sites (Nye *et al.*, 1992). Second, circular dichroism difference spectra of DNA obtained in the presence and absence of Ets-1ΔN331 indicate that the structure of the nucleic acid is perturbed by the protein (Petersen *et al.*, 1995). Detailed crystallographic or NMR studies will be necessary to describe the nature of these conformation changes and to determine the orientation of the ETS domain wHTH on cognate binding sites.

Alterations in the DNA binding affinity and transactivation properties of the v-Ets oncoprotein have been attributed to a single point mutation of Ile401 to Val found within the ETS domain (Golay *et al.*, 1988; Hahn and Wasylyk, 1994; Soudant *et al.*, 1994). This residue is located at the beginning of strand S3 and contributes to the hydrophobic core of the ETS domain. Thus the amino acid substitution is likely to perturb the structure of the protein, as opposed to changing contacts with DNA directly.

The C-terminus of Ets-1

Although not part of the highly conserved ETS domain, the C-terminal 25 residues contribute significantly to the overall structure of Ets-1ΔN331 (Figures 1 and 3). These residues follow from the β-sheet, forming an extended loop and the final helix H4. This helix, comprised of Glu428–Leu434, has an amphipathic character and lies anti-parallel to helix H1. Trp338 plays a key role in the packing of helices H1 and H4. Several important contacts are also made by Leu418 and Tyr424 in the loop region with the non-conserved Trp361 in strand S2 and Leu342 in helix H1. A minimal truncation mutant of murine Ets-1 (residues 331–415) that lacks the C-terminal tail is fully active for DNA binding, yet shows limited solubility (Q.Xu and B.J.Graves, unpublished). Therefore, this sequence, while not required for DNA recognition, influences the behaviour of the Ets-1 ETS domain as a structural module.

The C-terminal residues are also implicated in the regulation of DNA binding activity (Hagman and Grosschedl, 1992; Lim *et al.*, 1992; Hahn and Wasylyk, 1994). Truncation of the C-terminus within the context of the full-length protein increases the DNA binding affinity of Ets-1. Equilibrium and kinetic binding studies, along

with proteolysis data, show that the C-terminal residues allosterically repress DNA binding by acting in combination with inhibitory residues immediately N-terminal to the ETS domain of Ets-1 (M.Jonsen, J.M.Petersen, Q.Xu and B.J.Graves, submitted). The tertiary structure of Ets-1ΔN331 places the N- and C-termini within close proximity to one another, consistent with a direct interaction between amino and carboxyl inhibitory regions (Figures 1 and 3). Furthermore, the juxtaposition of helices H1 and H4 places the C-terminal inhibitory region in contact with the ETS domain, in a position to mediate inhibition of DNA binding by an allosteric mechanism. In our NMR-derived structure of Ets-1ΔN331, helix H4 is locally well defined, yet not positioned precisely within the tertiary fold. It is possible that the C-terminal sequence is conformationally mobile in the absence of additional intramolecular interactions. The effects of the N-terminal inhibitory region on the structure of the ETS domain and the C-terminus of Ets-1 are being explored (Skalicky *et al.*, 1995).

The importance of the C-terminus in regulating DNA binding is also apparent from studies of the oncogenic variant of Ets-1. In addition to the point mutation described earlier, v-Ets contains a substitution of the C-terminal 12 amino acids of c-Ets-1 with a completely different 16 amino acid sequence (Lautenberger and Papas, 1993; Leprince *et al.*, 1993). The C-terminal sequence of murine Ets-1 is ^{428}ELHAMLDVKPDAD^{440}, with H4 underlined, while that of v-Ets is ^{428}EHSSASGLTSSMACSSF^{445}. DNA binding studies have shown that v-Ets has a higher DNA affinity than Ets-1 (Lim *et al.*, 1992; Hahn and Wasylyk, 1994). Replacement of the 12 C-terminal residues of Ets-1 with the 16 terminal residues of v-Ets also increases DNA binding activity relative to Ets-1 (Hagman and Grosschedl, 1992). We have analysed the C-terminal sequence of the viral protein using a secondary structure prediction program (Rost and Sander, 1993). These predominantly polar amino acids are not expected to form an α-helix and, furthermore, should not pack against the ETS domain in the same manner as observed with the C-terminus of Ets-1ΔN331. Any interactions between helix H4 and either the wHTH motif or the N-terminal inhibitory sequences would be absent in the v-Ets polypeptide, thus relieving inhibition of DNA binding.

Summary

From the structure determination of Ets-1ΔN331 described in this report, we have shown that the murine Ets-1 ETS domain is a wHTH DNA binding motif. Analogous to other wHTH proteins, DNA recognition is likely mediated by the HTH motif and augmented by possible contacts from helix H1 and the wing component found in the β-sheet. This structure provides a framework for understanding the binding of specific promoter sequences by the *ets* family of regulatory proteins. The second major finding of this study is that the C-terminal residues of Ets-1ΔN331, which are implicated in the autoinhibition of Ets-1, adopt a helical conformation. This helix is positioned near the N-terminus of the ETS domain, suggesting a direct structural coupling of the N- and C-terminal inhibitory sequences with the intervening wHTH motif to repress DNA binding by native Ets-1. A variety of regulatory events could release the ETS domain from the negative influence of these flanking sequences, including post-translational modifications or association with protein partners. This NMR analysis has provided a starting point to begin elucidating the structural and mechanistic aspects of intramolecular inhibition and to define the role played by this phenomenon in the biological function of the Ets-1 transcription factor.

Materials and methods

Protein samples

An *E.coli* expression system was used to produce uniformly and selectively ^{13}C-, ^{15}N- and ^{2}H-labelled Ets-1ΔN331 (Donaldson *et al.*, 1994). Selectively ring-deuterated proteins were prepared from a synthetic media containing 100 mg/l of two of L-δ_1,ε_2, $\zeta_{1,2}$,η_2-[$^2H_5$]tryptophan, L-$\delta_{1,2}$,$\varepsilon_{1,2}$, ζ-[$^2H_5$]phenylalanine, or L-$\delta_{1,2}$,$\varepsilon_{1,2}$-[$^2H_4$]tyrosine (Cambridge Isotope Laboratories and Isotec Inc.) (McIntosh and Dahlquist, 1990; McIntosh *et al.*, 1990). Fractionally ^{13}C-labelled Ets-1ΔN331 was prepared using minimal media containing 10% (0.3 g/l) [$^{13}C_6$]glucose and 90% (2.7 g/l) unenriched glucose (Neri *et al.*, 1989).

All samples were 0.6–0.8 mM protein in 20 mM sodium phosphate (pH 6.5), 500 mM sodium chloride, 0.01% sodium azide, 10 mM dithiothreitol (DTT), in 10 or 99% D_2O. An examination of the surface residues of Ets-1ΔN331 reveals a dipolar character to this protein. Basic residues cluster around the helix H3 and the preceding turn, while acidic residues cluster on the opposite face of the molecule near helix H1. The localized basic and acidic patches may provide an explanation for the need to use high ionic strength conditions to prevent aggregation of Ets-1ΔN331. The two non-conserved cysteine residues in Ets-1ΔN331, Cys350 and Cys416, are exposed on surface loops of the protein. These cysteines are susceptible to oxidation by Ellman's reagent [5,5′-dithiobis(2-nitrobenzoic acid); data not shown] and were maintained in the reduced form by the inclusion of fresh DTT in all sample buffers.

NMR experiments

NMR spectra were recorded at 20°C on a Varian Unity 500 spectrometer equipped with a pulsed-field gradient accessory. NMR data were processed and analysed using Felix v2.30 (Biosym Technologies, San Diego, CA) and NMRpipe/PIPP software (F.Delaglio and D.Garrett, NIDDK, National Institutes of Health, Bethesda, MD). The resonances from side chain aliphatic ^{1}H and ^{13}C nuclei were identified using HCCH-TOCSY experiments with 8 ms and 16 ms DIPSI-3 mixing periods recorded on a sample of uniformly ^{15}N/^{13}C-labelled protein in H_2O (Kay *et al.*, 1993). These assignments were verified with sensitivity-enhanced versions of the H(CCO)NH and C(CO)NH experiments using 8 ms DIPSI-3 mixing periods (Grzesiek *et al.*, 1993; Muhandiram and Kay, 1994). The methyl groups of leucine and valine were assigned stereospecifically from gradient ^{1}H-^{13}C HSQC spectra of 10% fractionally ^{13}C-labelled protein (Neri *et al.*, 1989; Wider and Wüthrich, 1993). Aromatic ring proton resonances were assigned using 2-D DQF-COSY, TOCSY and NOESY experiments recorded on Ets-1ΔN331 in 99% D_2O in which two of tryptophan, tyrosine and phenylalanine were selectively deuterated (McIntosh *et al.*, 1990). Aromatic ring carbon resonances were identified from constant time ^{1}H-^{13}C HSQC, (Hβ)Cβ(CγCδ)Hδ and (Hβ)Cβ(CγCδCε)Hε experiments (Santoro and King, 1992; Vuister and Bax, 1992; Yamazaki *et al.*, 1993).

NOE distance constraints were measured from sensitivity-enhanced 3-D ^{15}N-NOESY-HSQC (125 ms mixing period) and simultaneous ^{15}N/^{13}C-NOESY-HSQC (50 and 150 ms) experiments (Pascal *et al.*, 1994; Zhang *et al.*, 1994). In addition, many critical long distance constraints involving aromatic protons were obtained using 2-D ^{1}H-^{1}H NOESY spectra (125 ms) recorded with samples of Ets-1ΔN331 in 99% D_2O with selectively deuterated aromatic rings. $^3J_{HN\text{-}H\alpha}$ couplings were measured with the HMQC-J experiment (Kay and Bax, 1990), using software provided by Dr L.E.Kay (University of Toronto).

Structure generation

All structure calculations were performed using X-PLOR 3.1 and protocols outlined in the X-PLOR manual (Brünger, 1992). A total of 229 intraresidue, 383 short range ($1<|i-j|<4$), and 123 long range ($|i-j|>4$) distance restraints, 29 hydrogen bonds, and 77 φ angle restraints were used in structure calculations. Interproton distance restraints were assigned to three strengths following a square-well potential energy function: weak, 1.8–5.0 Å, medium; 1.8–3.5 Å; strong 1.8–2.9 Å. A

correction of 0.5 Å was added to the upper bounds of restraints involving methyl groups. Prochiral H^{β} groups, as well as the aromatic rings of phenylalanine and tyrosine, were treated as pseudo-atoms. Based on $^{3}J_{HN\text{-}H\alpha}$ couplings, ϕ torsion angles were restrained to three regimes following a quadratic potential energy function: <7 Hz, $-60° \pm 40°$; (8 Hz <J<9 Hz), $-120° \pm 60°$; >9 Hz, $-140° \pm 40°$. Main chain hydrogen bonding restraints were included for residues showing protection from amide hydrogen exchange as well as dihedral angles and NOE patterns diagnostic of α-helical or β-sheet secondary structures (Donaldson *et al.*, 1994). No medium or long range constraints were observed for the four N-terminal residues 331–334, suggesting a disordered conformation in solution. Therefore, these residues were omitted from the structure calculations.

Although distance geometry methods produced similar results, an ensemble of structures was generated most directly using the following method: (i) the Ets-1 sequence was aligned to the *K.lactis* HSF sequence using regions of amino acid identity and secondary structure as cues (Harrison *et al.*, 1994). (ii) For each residue in Ets-1 with a counterpart in HSF, N, C^{α}, C^{β} and C′ coordinates were extracted from the HSF structure. (iii) All other side chain atoms and loop regions were given default coordinates of 9999.0 Å. (iv) This file, which now resembled output from a sub-embedded distance geometry protocol, was submitted to standard restrained simulated annealing and refinement protocols (Nilges *et al.*, 1988).

A total of 50 simulated annealing structures were calculated. The top 20 structures that had no NOE violations >0.5 Å, no dihedral angle restraint violations >5°, and a low target energy were selected for refinement. An average structure was calculated and subjected to restrained regularization according to standard X-PLOR protocols. Using NOE and dihedral force constants of 50 kcal/mol/Å and 200 kcal/mol/rad^2, respectively, the average X-PLOR target energies in kcal/mol for the ensemble after final refinement were: total, 167.9 ± 6.5; bonds, 9.94 ± 0.28; angles, 64.5 ± 0.2; impropers, 11.9 ± 0.3; van der Waals, 56.8 ± 2.9; NOE, 23.5 ± 2.8; dihedral angles, 1.36 ± 0.02. The atomic co-ordinates have been submitted to the Brookhaven Protein Data Bank.

Structural analyses

The average structure was assessed with Quanta (Molecular Simulations; Burlington, MA) and PROCHECK (Laskowski *et al.*, 1988). The secondary structure of Ets-1ΔN331 was defined as previously reported (Donaldson *et al.*, 1994) using information from NMR secondary chemical shifts, $^{3}J_{HN\text{-}H\alpha}$ coupling constants and patterns of interresidue short range NOEs, combined with the main chain dihedral angles observed in the ensemble of calculated structures. The angular order parameters, Sφ and Sψ, were calculated from the ensemble of 20 simulated annealing structures according to Hyberts *et al.* (1992) using software generously provided by G.Wagner (Harvard Medical School). Interhelical angles were measured using the *interhx* module of the *ribbons* suite of programs (Carson, 1991). Interhelical angles are defined such that 0° is parallel and 180° anti-parallel. A comprehensive comparison of interhelical angles and r.m.s. differences between wHTH proteins may be found in Vuister *et al.* (1994b).

Acknowledgements

We are indebted to Dr L.E.Kay for providing the NMR pulse sequences used in this study. We thank Drs J.Skalicky, S.Pascal and T.Alber for valuable advice, and Dr S.Fesik for providing the co-ordinates of the Fli-1 ETS domain. This work was supported by grants from the National Cancer Institute of Canada, with funds from the Canadian Cancer Society (to L.P.M.), the National Institutes of Health GM 38663/CA 42014, and the University of Utah Cancer Center (to B.J.G). Instrument support from the Protein Engineering Network of Centres of Excellence (to L.P.M.) is gratefully acknowledged.

References

Bosselut,R., Levin,J., Adjadj,E. and Ghysdael,J. (1993) A single amino acid substitution in the Ets domain alters core DNA binding specificity of Ets1 to that of the related transcription factors Elf1 and E74. *Nucleic Acids Res.*, **21**, 5184–5191.

Brünger,A.T. (1992) *X-PLOR 3.1: A System for X-Ray Crystallography and NMR*. Yale University, New Haven, CT.

Brennan,R. (1993) The winged-helix DNA-binding motif: another helix–turn–helix takeoff. *Cell*, **74**, 773–776.

Bussiere,D.E., Bastia,D. and White,S.W. (1995) Crystal structure of the replication terminator protein from *B.subtilis* at 2.6 Å. *Cell*, **80**, 651–660.

Carson,M. (1991) *Ribbons 2.0 Manual*. University of Alabama at Birmingham, Birmingham, AL.

Clark,K., Halay,E., Lai,E. and Burley,S. (1993) Co-crystal structure of the HNF-3/forkhead DNA-recognition motif resembles histone H5. *Nature*, **364**, 412–420.

Clubb,R., Omichinski,J., Savilahti,H., Mizuuchi,K., Gronenborn,A. and Clore,G. (1994) A novel class of winged helix–turn–helix protein: the DNA-binding domain of Mu transposase. *Structure*, **2**, 1041–1048.

Damberger,F., Pelton,J., Harrison,C., Nelson,H. and Wemmer,D. (1994) Solution structure of the DNA-binding domain of the heat shock transcription factor determined by multidimensional heteronuclear magnetic resonance spectroscopy. *Protein Sci.*, **3**, 1806–1821.

Degnan,B., Degnan,S., Naganuma,T. and Morse,D. (1993) The ets multigene family is conserved throughout the metazoa. *Nucleic Acids Res.*, **21**, 3479–3484.

Donaldson,L., Petersen,J., Graves,B. and McIntosh,L. (1994) Secondary structure of the ETS domain places murine Ets-1 in the superfamily of winged helix–turn–helix DNA-binding proteins. *Biochemistry*, **33**, 13509–13516.

Fisher,R.F., Mavrothalassitis,G., Kondoh,A. and Papas,T.S. (1991) High-affinity DNA–protein interactions of the cellular ETS1 protein: the determination of the ETS binding motif. *Oncogene*, **6**, 2249–2254.

Fisher,R., Fivash,M., Casas-Finet,J., Erickson,J., Kondoh,A., Bladen,S., Fisher,C., Watson,D. and Papas,T. (1994) Real-time DNA binding measurements of the ETS1 recombinant oncoproteins reveal significant kinetic differences between the p42 and p51 isoforms. *Protein Sci.*, **3**, 257–266.

Fogh,R., Ottleben,G., Ruterjans,H., Schnarr,M., Boelens,R. and Kaptein,R. (1994) Solution structure of the LexA repressor DNA binding domain determined by ^{1}H NMR spectroscopy. *EMBO J.*, **13**, 3936–3944.

Golay,J., Introna,M. and Graf,T. (1988) A single point mutation in the v-*ets* oncogene affects both erythroid and myelomonocytic cell differentiation. *Cell*, **55**, 1147–1158.

Grzesiek,S., Anglister,J. and Bax,A. (1993) Correlation of backbone amide and aliphatic side chain resonances in $^{13}C/^{15}N$ proteins by isotropic mixing of ^{13}C magnetization. *J. Magn. Reson. Ser. B*, **101**, 114–119.

Hagman,J. and Grosschedl,R. (1992) An inhibitory carboxyl-terminal domain in Ets-1 and Ets-2 mediates differential binding of ETS family factors to promoter sequences of the *mb-1* gene. *Proc. Natl Acad. Sci. USA*, **89**, 8889–8893.

Hahn,S. and Wasylyk,B. (1994) The oncoprotein v-Ets in less selective in DNA binding than c-Ets-1 due to the C-terminal sequence change. *Oncogene*, **9**, 2499–2512.

Harrison,C., Bohm,A. and Nelson,H. (1994) Crystal structure of the DNA binding domain of the heat shock transcription factor. *Science*, **263**, 224–226.

Henikoff,S. and Heinkoff,J.G. (1992) Amino acid substitution matrices from protein blocks. *Proc. Natl Acad. Sci. USA*, **89**, 10915–10919.

Hubl,S., Owens,J. and Nelson,H. (1994) Mutational analysis of the DNA-binding domain of yeast heat shock transcription factor. *Nature Struct. Biol.*, **1**, 615–620.

Hyberts,S.G., Goldberg,M.S., Havel,T.F. and Wagner,G. (1992) The solution structure of eglin c based on measurements of many NOEs and coupling constants and its comparison with X-ray structures. *Protein Sci.*, **1**, 736–751.

Janknecht,R. and Nordheim,A. (1993) Gene regulation by Ets proteins. *Biochim. Biophys. Acta*, **1155**, 346–356.

Janknecht,R., Zinck,R., Ernst,W. and Nordheim,A. (1994) Functional dissection of the transcription factor Elk-1. *Oncogene*, **9**, 1273–1278.

Karim,F. *et al.* (1990) The ETS-domain: a new DNA-binding motif that recognizes a purine-rich core DNA sequence. *Genes Dev.*, **4**, 1451–1453.

Kay,L. and Bax,A. (1990) New methods for the measuring of NH-C^{α}H coupling constants in ^{15}N-labelled proteins. *J. Magn. Reson.*, **86**, 110–126.

Kay,L., Xu,G.-Y., Singer,A., Muhandiram,D. and Forman-Kay,J. (1993) A gradient-enhanced HCCH-TOCSY experiment for recording side chains ^{1}H and ^{13}C correlations in H_2O samples of proteins. *J. Magn. Res.*, **101**, 333–337.

Kraulis,P. (1991) MOLSCRIPT: a program to produce both detailed and schematic plots of protein structures. *J. Appl. Crystallogr.*, **24**, 946–950.
Laskowski,R., MacArthur,M., Moss,D. and Thornton,J. (1988) PROCHECK: a program to check the stereochemical quality of protein structures. *J. Appl. Crystallogr.*, **26**, 283–291.
Lautenberger,J. and Papas,T. (1993) Inversion of a chicken *ets-1* proto-oncogene segment in avian leukemia virus E26. *J. Virol.*, **67**, 610–612.
Lautenberger,J., Burdett,L., Gunnell,M., Qi,S., Watson,D., O'Brien,S. and Papas,T. (1992) Genomic dispersal of the *ets* gene family during metazoan evolution. *Oncogene*, **7**, 1713–1719.
Leprince,D., Gegonne,A., Coll,J., de Taisne,C., Schneeberger,A., Lagrou,C. and Stehlin,D. (1983) A putative second cell-derived oncogene of the avian leukaemia retrovirus E26. *Nature*, **306**, 395–397.
Leprince,D., Crepieux,P. and Stehelin,D. (1992) c-ets-1 DNA binding to the PEA3 motif is differentially inhibited by all the mutations found in v-ets. *Oncogene*, **7**, 9–17.
Leprince,D., Crepieux,P., Laudet,V., Flourens,A. and Stehelin,D. (1993) A new mechanism of oncogenic activation: E26 retroviral v-*ets* oncogene has inverted the C-terminal end of the transcription factor c-ets-1. *Virology*, **194**, 855–857.
Liang,H., Olejniczak,E., Mao,X., Nettesheim,D., Yu,L., Thompson,C. and Fesik,S. (1994a) The secondary structure of the ets domain of human Fli-1 resembles that of the helix–turn–helix DNA-binding motif of the *Escherichia coli* catabolite gene activator protein. *Proc. Natl Acad. Sci. USA*, **91**, 11655–11659.
Liang,H., Mao,X., Olejniczak,E.T., Nettesheim,D.G., Yu,L., Meadows,R.P., Thompson,C.B. and Fesik,S.W. (1994b) Solution structure of the Ets domain of Fli-1 when bound to DNA. *Nature Struct. Biol.*, **1**, 871–875.
Lim,F., Kraut,N., Frampton,J. and Graf,T. (1992) DNA binding by c-Ets-1, but not v-Ets, is repressed by an intramolecular mechanism. *EMBO J.*, **11**, 643–652.
Macleod,K., Leprince,D. and Stehelin,D. (1992) The *ets* gene family. *Trends Biochem. Sci.*, **17**, 251–256.
Mavrothalassitis,G., Fisher,R.J., Smyth,F., Watson,D.K. and Papas,T.S. (1994) Structural inferences of the ETS1 DNA-binding domain determined by mutational analysis. *Oncogene*, **9**, 425–435.
McIntosh,L. and Dahlquist,F. (1990) Biosynthetic incorporation of ^{15}N and ^{13}C for assignment and interpretation of nuclear magnetic resonance spectra of proteins. *Q. Rev. Biophys.*, **23**, 1–38.
McIntosh,L., Wand,A., Lowry,D., Redfield,A. and Dahlquist,F. (1990) Assignment of the backbone ^{1}H and ^{15}N NMR resonances of bacteriophage T4 lysozyme. *Biochemistry*, **29**, 6341–6362.
Muhandiram,D. and Kay,L. (1994) Gradient-enhanced triple-resonance three-dimensional NMR experiments with improved sensitivity. *J. Magn. Reson., Ser. B*, **103**, 203–216.
Neri,D., Szyperski,T., Otting,G., Senn,H. and Wüthrich,K. (1989) Stereospecific nuclear magnetic resonance assignments of the methyl groups of valine and leucine in the DNA-binding domain of the 434 repressor by biosynthetically directed fractional ^{13}C labelling. *Biochemistry*, **28**, 751–7516.
Nilges,M., Gronenborn,A.M., Brünger,A.T. and Clore,G.M. (1988) Determination of three-dimensional structures of proteins by simulated annealing with interproton distance restraints. Application to crambin, potato carboxypeptidase inhibitor and barley serine proteinase inhibitor 2. *Protein Engng*, **2**, 27–38.
Nunn,M. and Hunter,T. (1989) The ets sequence is required for induction of erythroblastosis in chickens by avian retrovirus E26. *J. Virol.*, **63**, 398–402.
Nunn,M., Seeburg,P., Moscovici,C. and Duesberg,P. (1983) Tripartite structure of the avian erythroblastosis virus E26 transforming gene. *Nature*, **306**, 391–397.
Nye,J., Petersen,J., Gunther,C., Jonsen,M. and Graves,B. (1992) Interaction of murine Ets-1 with GGA-binding sites establishes the ETS domain as a new DNA-binding motif. *Genes Dev.*, **6**, 975–990.
Pascal,S.M., Muhandiram,D.R., Yamazaki,T., Kay,J.D.F. and Kay,L.E. (1994) Simultaneous acquistion of ^{15}N and ^{13}C-edited NOE spectra of proteins dissolved in H_2O. *J. Magn. Reson.*, **103**, 197–201.
Petersen,J.M., Skalicky,J.J., Donaldson,L.W., McIntosh,L.P., Alber,T. and Graves,B.J. (1995) Modulation of transcription factor Ets-1 DNA binding: DNA induced unfolding of an α helix. *Science*, **269**, 1866–1869.
Pongubala,J.M., Nagulapalli,S., Klemsz,M.J., McKercher,S.R., Maki,R.A. and Atchison,L. (1992) PU.1 recruits a second nuclear factor to a site important for immunoglobulin kappa 3′ enhancer activity. *Mol. Cell. Biol.*, **12**, 368–378.
Qiu,X., Verlinde,C., Zhang,S., Schmitt,M., Holmes,R. and Hol,W. (1995) Three-dimensional structure of the diphtheria toxin repressor in complex with divalent cation co-repressors. *Structure*, **3**, 87–101.
Ramakrishnan,V., Finch,J., Graziano,V., Lee,P. and Sweet,R. (1993) Crystal structure of globular domain of histone H5 and its implications for nucleosome binding. *Nature*, **362**, 219–223.
Rost,B. and Sander,C. (1993) Prediction of protein structure at better than 70% accuracy. *J. Mol. Biol.*, **232**, 584–599.
Santoro,J. and King,G.C. (1992) A constant-time 2D overbodenhausen experiment for inverse correlation of isotopically enriched species. *J. Magn. Reson.*, **97**, 202–207.
Schultz,S., Shields,G. and Steitz,T. (1991) Crystal structure of a CAP–DNA complex: the DNA is bent by 90°. *Science*, **253**, 1001–1007.
Skalicky,J., Donaldson,L., Petersen,J., Graves,B. and McIntosh,L. (1995) Structural coupling of the inhibitory regions flanking the ETS domain of murine Ets-1. *Protein Sci.*, in press.
Soudant,N., Albagli,O., Dhordain,P., Flourens,A., Stehelin,D. and Leprince,D. (1994) A residue of the ETS domain mutated in the v-*ets* oncogene is essential for the DNA-binding and transactivating properties of the ETS-1 and ETS-2 proteins. *Nucleic Acids Res.*, **22**, 3871–3879.
Szyperski,T., Neri,D., Leiting,B., Otting,G. and Wüthrich,K. (1992) Support of ^{1}H NMR assignments in proteins by biosynthetically directed fractional ^{13}C-labeling. *J. Biomol. NMR*, **2**, 323–334.
Thompson,C.C., Brown,T.A. and McKnight,S.L. (1991) Convergence of Ets- and notch-related structural motifs in a heteromeric DNA binding complex. *Science*, **253**, 762–768.
Vuister,G.W. and Bax,A. (1992) Resolution enhancement and spectral editing of uniformly ^{13}C-enriched proteins by homonuclear broadband ^{13}C decoupling. *J. Magn. Reson.*, **98**, 428–435.
Vuister,G., Kim,S.-J., Wu,C. and Bax,A. (1994a) NMR evidence for similarities between the DNA-binding regions of *Drosophila melanogaster* heat shock factor and the helix–turn–helix and HNF-3/forkhead families of transcription factors. *Biochemistry*, **33**, 10–16.
Vuister,G., Kim,S.-J., Orosz,A., Marquardt,J., Wu,C. and Bax,A. (1994b) Solution structure of the DNA-binding domain of *Drosophila* heat shock transcription factor. *Nature Struct. Biol.*, **1**, 605–613.
Wasylyk,B., Hahn,S. and Giovane,A. (1993) The Ets family of transcription factors. *Eur. J. Biochem.*, **211**, 7–18.
Wasylyk,C., Kerckaert,J.-P. and Wasylyk,B. (1992) A novel modulator domain of Ets transcription factors. *Genes Dev.*, **6**, 965–974.
Wider,G. and Wüthrich,K. (1993) A simple experimental scheme using pulsed field gradients for coherence-pathway rejection and solvent suppression in phase-sensitive heteronuclear correlation spectra. *J. Magn. Reson.*, **102**, 239–241.
Wilson,K., Shewchuk,L., Brennan,R., Otsuka,A. and Matthews,B. (1992) *Escherichia coli* biotin holoenzyme synthetase/bio repressor crystal structure delineates the biotin- and DNA-binding domains. *Proc. Natl Acad. Sci. USA*, **89**, 9257–9261.
Woods,D.B., Ghysdael,J. and Owen,M.J. (1992) Identification of nucleotide preferences in DNA sequences recognized specifically by c-Ets-1 protein. *Nucleic Acids Res.*, **20**, 699–704.
Yamazaki,T., Forman-Kay,J.D. and Kay,L. (1993) Two-dimensional NMR experiments for correlating $^{13}C^{\beta}$ and $^{1}H^{\delta/\epsilon}$ chemical shifts of aromatic residues in ^{13}C-labelled proteins via scalar couplings. *J. Am. Chem. Soc.*, **115**, 11054–11055.
Zhang,O., Kay,L.E., Olivier,J.P. and Forman-Kay,J.D. (1994) Backbone ^{1}H and ^{15}N resonance assignments of the N-terminal SH3 domains of drk in folded and unfolded states using enhanced-sensitivity pulsed field gradient NMR techniques. *J. Biomol. NMR*, **4**, 845–858.

Received on August 4, 1995; revised on September 25, 1995